Vietnam Journal of Science and Technology ***61*** *(2) (2023) 291-301*

doi:10.15625/2525-2518/17417

Image compression in all-optical domain using one 6×6 multimode interference coupler

Bui Thi Thuy[1], Le Trung Thanh[2, *]

[1]*FPT University, Education Zone, Hoa Lac Hi-tech Park, km 29, Thang Long Boulevard, Thach Hoa, Thach That, Ha Noi, Viet Nam*

[2]*International School (VNU-IS), Vietnam National University, No.144 Xuan Thuy, Cau Giay, Ha Noi, Viet Nam*

[*]Emails: *thanh.le@vnu.edu.vn*

Received: 6 August 2022; Accepted for publication: 21 September 2022

Abstract. We present a new method for image compression using the Haar wavelet transform (HWT) in all-optical domain. The proposed architecture is based on the optical Haar wavelet transform using only one 6×6 multimode interference (MMI) coupler. By locating the positions of input and output waveguides and optimizing design of the width and length of the MMI, the expected matrix of the Haar transform is obtained. The new hardware architecture is suitable for directly integrating with digital cameras for image processing. The processing of images therefore is at very high speed. Our method can also be applied to data compression in big data analytics. Our structure can provide a large fabrication tolerance which is compatible with the CMOS existing technology. Our simulations show that the length variation of ± 2 µm still keeps the output powers unchanged. We have simulate successfully the use of the proposed HWT to compress cameraman image with the compressed ratios of 20, 30, 50 % with MSE and PSNR from 0.1 - 0.3 and 62 - 67 dB, respectively.

Keywords: image compression, Haar wavelet transform, signal transform, optical signal processing, optical image processing.

Classification numbers: 2.1.1, 2.4.1, 4.2.3, 4.10.2

1. INTRODUCTION

Data compression supports to reduce the use of many expensive resources. In recent years, the implementation of artificial intelligence (AI) algorithms has still relied on the electronic computing systems. The original neural networks based on conventional CPU (Central Processing Unit) architectures for computation, but it was unable to handle the demands of very big data [1]. Moreover, the parallel computing efficiency was low and it must be replaced by GPU (Graphics Processing Unit) with parallel computing capability. In practice, GPU promotes the development of deep learning and AI. Practical applications such as image classification, face recognition based on deep learning algorithms require a large amount of computing resources. However, the traditional deep learning has a bottleneck due to electrical signals at high speed processing [2]. The researchers are attempting to find out other methods to solve electronic defects. One of the most promising answers to solve problems with data transportation is photonic interconnects or all-optical computing systems [3]. When GPUs are used for applications such as facial recognition, image classification, deep learning applications, GPUs will transform the optical information into electrical signals. Then the chips process those signals on a schedule, with a clock directing them to perform certain tasks at specific times. At practically every level of the computing hierarchy, photonic linkages have already supplanted metallic ones for the transfer of information at light speed, and they are currently being investigated for integration at the chip size.

In recent years, the demain for high speed signal processing of images, big data is required and causes the serious bottleneck in electronic domain [4]. By implementing the signal procesisng tasks such as buffering, data compression to optical domain, we can achieve a significant reduction in the electronic computing and processing systems. In particular, signal transforms applied to data signal procesisng take a significant amount of processing power on CPUs and FPGAs (Field Programmable Gate Arrays) [5].

In order to keep data processing such as image and video data in the all-optical domain, all-optical computing systems and optical micro-processors are being attractive [6]. The important key is the possibility of implementation of the real time functionalities [7]. Therefore, a whole new approach of computing has been developed, in which photons are employed as the information carrier rather than electrons. Since the development of laser, the possibility that optics may replace electronics in digital image processing and computation has been investigated.

The architectural concepts include everything from implemented programmable photonic logic arrays using smart pixels, and special purpose cellular image processing, to digital photonic computers based on non-linear logic with new types of optical logic gates. Image capture, processing, and characterization at high speeds have revolutionized industries such as high throughput microscopy and machine vision. Traditionally, image capture is conducted using CMOS (Complementary Metal-Oxide-Semiconductor) image sensors or CCDs (Charge Coupled Device) in the electrical domain [8]. Utilizing optical computing systems, recent research has focused on addressing these weaknesses. However, these systems generate a large quantity of data that must be processed and stored, and although photonic time stretch is a very effective tool for picture acquisition.

Image compression is an essential aspect of image processing that may be accomplished via discrete transforms, namely the Haar transform. With the premise that accuracy loss is acceptable, an image compressor is a vital technique that may significantly aid in reducing file size and bandwidth use. The sizes of the arrays are specified as powers of two. The original resolution of the photos is mathematically transformed to the next greater power of two, and the array sizes are initialized correspondingly. The Haar transform splits an image into components of high frequency and low frequency.

In the literature, the image processing and signal transforms in optical domain have been studied, but most of the research work is based on fiber optics [9] or Fourier optics [10]. These methods require a large size and cannot be integrated with photonic integrated circuits that can be embedded in the camera in the future. Image processing in integrated optics using meta-materials and optical waveguide circuits has been studied [5, 8]. These methods are based on directional couplers and 2×2 MMIs based on meta-materials or the Si_3N_4 platform. Such methods require complex fabrication steps.

This study proposes a new method based on only one 6×6 MMI coupler for image compression directly in all-optical domain for the first time. The architecture can be implanted in the AI camera for image processing before transmiting to the other networks. We design the hardware architecture on the Si_3N_4 material that suitable for both colour and gray images. Our proposed method has advantages of low loss, compactness, low fabrication tolerance and high speed.

2. THEORY OF THE HAAR WAVELET TRANSFORM FOR IMAGE COMPRESSION

The image array is split into two halves consisting of the low-pass element and the high-pass element. After transforming the image in the row, the image is then transformed along the column. Figure 1 shows the working principle of image compression based on discrete Haar wavelet transform (HT).

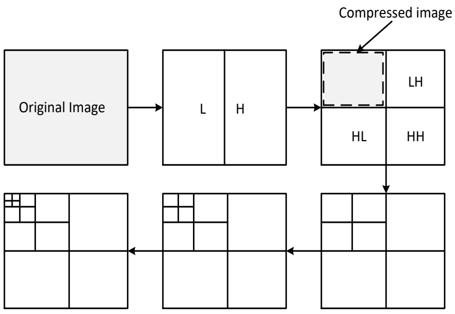

Figure 1. Principle of image compression based on Haar wavelet transform.

A principle of image processing based on pixel convolution is depicted in Figure 2 [7]. The mail is to handle images with fast signal processing, maintaining all functionalities in the optical domain.

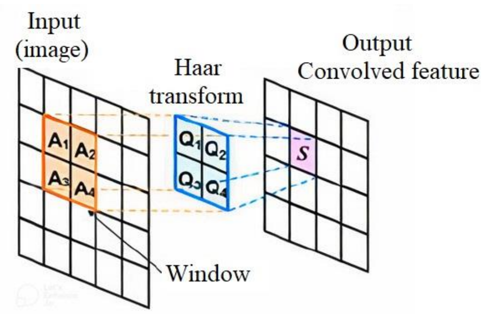

Figure 2. Image compression based on Haar wavelet transform implemented in optical domain.

In recent years, we have presented an approach to implement all-optical Haar wavelet transform using multimode interference (MMI) structure for the first time [11]. From this idea, the Haar transform using directional couplers in all-optical domain for image compression has been developed in recent years [8]. In this study we further develop the Haar wavelet transform for image processing applications. The silicon nitride working at the red, blue and green wavelength (532 nm, 635 nm and 405 nm) is used for the design. Our structure can be useful for high speed image processing and compression of big data. The new proposed method is advantageous of high speed, low loss and compatible with CMOS technology. The Haar wavelet transform decomposes a discrete signal into two sub-signals [12]. For a continuous signal, the wavelet transform of signal f(t) is expressed by [13]:

$$CWT_f(\tau,a)=\frac{1}{\sqrt{a}}\int f(t)h^*(\frac{\tau-a}{a})dt \quad (1)$$

where $h(t-\tau)/a$ is the mother wavelet with a shift and scale factor of τ and a, respectively. For a discrete signals, $a=2^j$, the mother wavelet is rewritten by:

$$h_{j,k}=2^{-j/2}h(2^{-j}t-k) \quad (2)$$

the wavelet transform for a discrete time signal f(n) then can be expressed by:

$$DWT_f(j,k)=\sum_n f(n)h_{j,k}(n) \quad (3)$$

For a discrete signal f with the length of N, the first running aversage and the difference are given by:

$$a^1=(a_1,a_2,...,a_{N/2}) \quad (4)$$

$$d^1=(d_1,d_2,...,d_{N/2}) \quad (5)$$

$$a_m=\frac{f_{2m-1}+f_{2m}}{\sqrt{2}},\ d_m=\frac{f_{2m-1}-f_{2m}}{\sqrt{2}}, \text{ for m=1, 2, 3,...,N/2}$$

The first order of the Haar transform is the mapping $f^{H_1}\mapsto H_1=(a^1,d^1)$. The Haar transform is based on the Haar function, which is periodic, orthogonal and complete. The first order Haar matrix is defined as

$$H_1=\frac{1}{\sqrt{2}}\begin{bmatrix}1 & 1\\ 1 & -1\end{bmatrix}. \quad (6)$$

3. HAAR TRANSFORM BASED ON 6×6 MMI COUPLER

The architecture to perform the HWT based on 6×6 MMI coupler in optical domain is presented in Figure 3. This structure can implement the 4-point Haar transform. For the first time, we show that the Haar transform matrix can be performed by using the 6×6 MMI in all-optical domain. The bock of 4 bits in image signals represented at input ports In1, In2, In3 and In4. The processed signals after the Haar transform are presented at output ports Out1, Out2, Out3, Out4.

Figure 3. Photonic circuit for implementing the 4-point Haar transform using 6x6 MMI coupler.

As mentioned earlier, the optical HT can be realized using optical structures [11]. The operation of optical MMI coupler is based on the self-imaging principle [14]. Self-imaging is a property of a multimode waveguide by which as an input field is reproduced in single or multiple images at periodic intervals along the propagation direction of the waveguide. In the multimode region, the 2-D scalar Helmholtz wave equation is defined as

$$\frac{\partial^2\psi}{\partial x^2}+\frac{\partial^2\psi}{\partial y^2}+\left[\frac{2\pi n(x,y)}{\lambda}\right]^2\psi=\beta^2\psi \tag{1}$$

where $\psi(x,y,z)=\sum_{\nu=0}^{M-1}c_\nu\psi_\nu(x,y)\exp(j(\omega t-\beta_\nu z))$; c_ν is the filed excitation coefficient; $\psi_\nu(x,y)$ is the modal field distribution; n(x,y) is the refractive index, ν is the mode number; λ is the optical wavelength and β is the propagation constant. In this study, the access waveguides are identical single mode waveguides. The input and output waveguides are located at [15]:

$$x_i=(i+1/2)\,W_{MMI}/N \tag{7}$$

In this study, we propose a 6×6 MMI coupler with a width of W_{MMI}, length of $L_{MMI}=1.5L_\pi$. The transfer matrix of the 6×6 MMI coupler is

$$\mathbf{S}=\frac{1}{\sqrt{2}}\begin{bmatrix} e^{j\frac{\pi}{4}} & 0 & 0 & 0 & 0 & e^{j\frac{3\pi}{4}} \\ 0 & e^{j\frac{\pi}{4}} & 0 & 0 & e^{j\frac{3\pi}{4}} & 0 \\ 0 & 0 & e^{j\frac{\pi}{4}} & e^{j\frac{3\pi}{4}} & 0 & 0 \\ 0 & 0 & e^{j\frac{3\pi}{4}} & e^{j\frac{\pi}{4}} & 0 & 0 \\ 0 & e^{j\frac{3\pi}{4}} & 0 & 0 & e^{j\frac{\pi}{4}} & 0 \\ e^{j\frac{3\pi}{4}} & 0 & 0 & 0 & 0 & e^{j\frac{\pi}{4}} \end{bmatrix} \tag{8}$$

As an example, the second Haar matrix is given below:

$$H_2=\begin{bmatrix} 1 & 1 & 1 & 0 \\ 1 & 1 & -1 & 0 \\ 1 & -1 & 1 & 1 \\ 1 & -1 & 0 & -1 \end{bmatrix} \tag{9}$$

The Haar transform matrix formed from the 6×6 MMI coupler can be expressed by

$$H_{6x6MMI}=\begin{bmatrix} \alpha e^{j\pm\delta} & \alpha e^{j\pm\delta} & \alpha e^{j\pm\delta} & 0 \\ \alpha e^{j\pm\delta} & \alpha e^{j\pm\delta} & -\alpha e^{j\pm\delta} & 0 \\ \alpha e^{j\pm\delta} & -\alpha e^{j\pm\delta} & \alpha e^{j\pm\delta} & \alpha e^{j\pm\delta} \\ \alpha e^{j\pm\delta} & -\alpha e^{j\pm\delta} & 0 & -\alpha e^{j\pm\delta} \end{bmatrix} \tag{10}$$

where α and δ are variations in amplitude and phase around 1 and 90 degree. In the next section, we show that our proposed architecture can provide a very low fabrication tolerance. As a result, the Haar transform can be implemented accurately.

4. RESULTS AND DISCUSSION

For numerical simulations, Si_3N_4 core waveguide working at visible wavelengths is used. The height and width of the waveguide are 170 nm and 1600 nm, respectively. The calculated effective refractive index is to be $n_{eff} = 1.7$. The numerical simulation results for the 6x6 MMI design are shown in Figure 6. Figure 4 shows the field propagation of pixel intensity level transmitting through the Haar transform based on 6×6 MMI coupler. The 3D EME (Expansion Mode Method) has been used for the simulation [16]. The matrix of the MMI is then put into the Python based code for image processing. The optimal length and width of the 6×6 MMI calculated to be 6360 µm and 36 µm. Figure 4 shows the signal propagation over the 6×6 MMI coupler for input signals at port 1, 2 and 3, respectively.

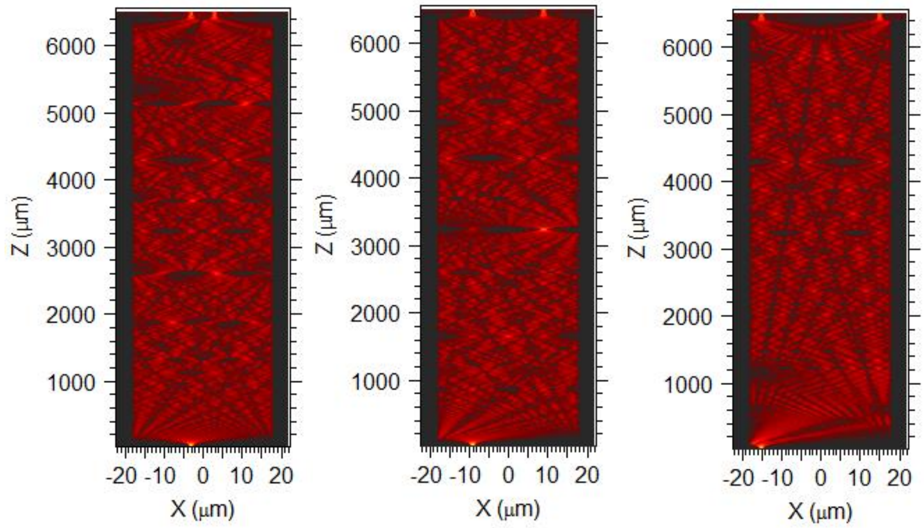

(a) (b) (c)

Figure 4 (a). Input signal at port 3 (b) input signal at port 2 and (c) input signal at port 1.

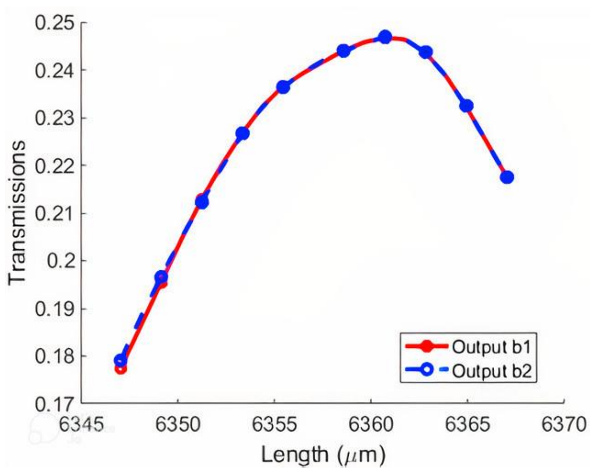

Figure 5. Powers at port 1 and 2 when input signal is at port 1 and port 2 with different lengths of the 6×6 MMI.

The normalized powers at output ports 1 and 2 when input signal is at port 1 and port 2 are shown in Figure 5. The simulations show that the length variation of ± 2 μm still keeps the output powers unchanged. This means that the fabrication tolerance of the proposed structure is high. The current CMOS fabrication technology for VLSI industry is feasible.

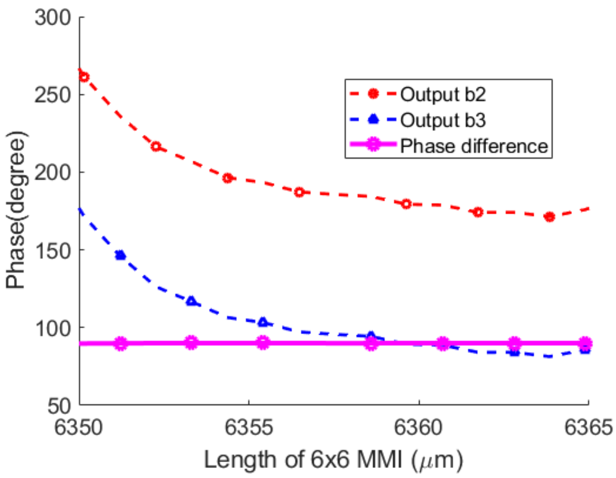

Figure 6. The phases at output ports 1 and 6 when input signal is at port 1.

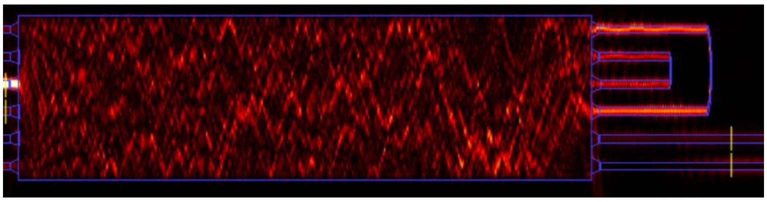

(a) input signals 1000

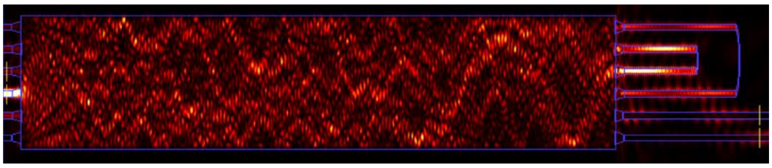

(b) input signals 0100

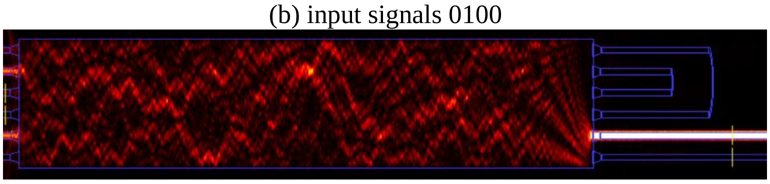

(c) input signals 0010

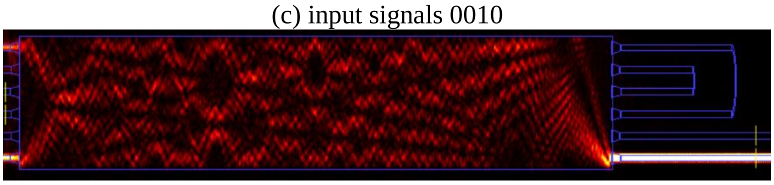

(d) input signals 0001

Figure 7. The 3D simulations for the 4-point Haar transform with different input signals (a) input signals "1-0-0-0", (b) input signals "0-1-0-0", (c) input signals "0-0-1-0" and (d) input signals "0-0-0-1".

Original image Compressed image

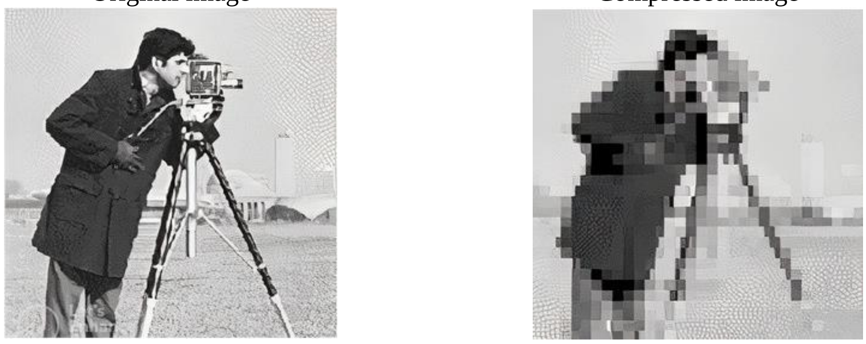

(a) "Camera man" image, CR = 20 %

Original image Compressed image

(b) "Camera man" image, CR = 30 %

Original image Compressed image

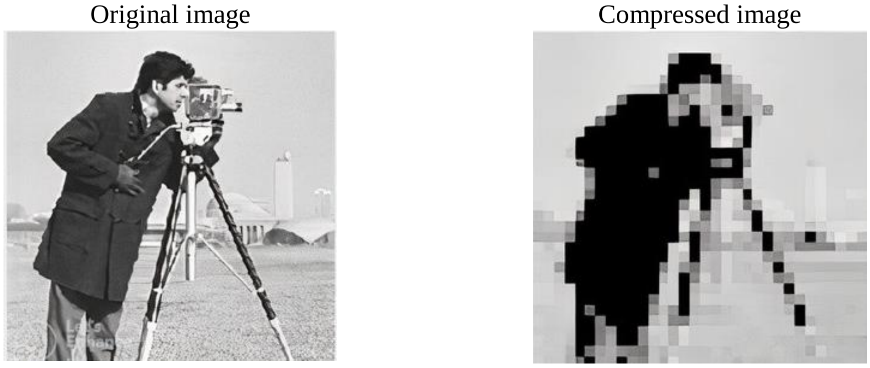

(c) "Camera man" image, CR = 50 %

Original image Compressed image

(d) "Camera man" image, CR = 0 %

Figure 8. Original and compressed images.

Next, we investigate the phase error of the Haar transform. The phases at output ports 1 and 6 when input signal is at port 1 are shown in Figure 6. The phase shift difference between port 1 and 6 is also presented in this simulation. The results show that the phase difference of 90 degree can be obtained over a length variation of 18 µm. This result provides a flexible design for the optical HT. The HT can be implemented extremely accurately using the CMOS fabrication technology.

Next we undertake the simulations for input image of the "camera man", 256×256 in size at different compressed ratios of 0 %, 20 %, 30 % and 50 % with the optical Haar Transform architecture designed above.

The simulation results are shown in Figure 8. The Haar transform is implemented in the optical domain. The original image of "camera men", which is used for image processing standard for comparison, is used for processing. The input image is imported from Python plaform. The matrix of the Haar transform is got from the optical numerical simulations.

As an example, we show the results for compressed images compared to the original image with different compressed ratios (CR) in Figure 10. Performance evaluation is based on the Mean Square Error (MSE) and Peak Signal to Noise Ratio (PSNR) calculation. The MSE between two images f and g (size MxN) can be expressed by

$$MSE = \frac{1}{MxN}\sum_{j=1}^{N}\sum_{k=1}^{M}\left[f(j,k) - g(j,k) \right]^2 \tag{11}$$

$$PSNR\ [dB] = 10 Log_{10}\left(\frac{255^2}{MSE}\right) \tag{12}$$

Table 1 presents the comparison of the MSE, PSNR, the images compressed by using the optical Haar transform.

Table 1. Image compression results for the camera man image.

CR (Compressed Ratio)	**PSNR (dB)**	**MSE**
20 %	67	0.0126
30 %	65	0.0223
50 %	62	0.0333
0 %	inf	0

5. CONCLUSIONS

This paper has presented a new approach for implementing image compression technique based on Haar wavelet transform using the 6×6 MMI coupler in all-optical domain. The proposed approach is useful for image processing and big data processing at extreme high speed. A large fabrication tolerance of ± 2 µm in length is achieved. The structure is based on only one MMI and it can provide a low loss and extreme compactness. The existing CMOS technology can be used for fabricating the device with one mask for fabrication steps. The proposed method can be integrated with the AI camera to implement image processing directly in the camera.

Acknowledgment. This research is funded by Vietnam national foundation for science and technology development (nafosted) under grant number 103.03-2018.354.

CRediT authorship contribution statement. Bui Thi Thuy: Methodology, Writing manuscript, Conceptualization, Formal analysis. Le Trung Thanh: Supervision, Conceptualization, Review and editing, Formal analysis.

Declaration of competing interest. The authors declare that they have no known competing financial interests or personal relationships that could have appeared to influence the work reported in this paper.

REFERENCES

1. Xu X., Tan M., Corcoran B., Wu J., Boes A., Nguyen T. G., Chu S. T., Little B. E., Hicks D. G., Morandotti R., Mitchell A., Moss D. J. - 11 TOPS photonic convolutional accelerator for optical neural networks, Nature. **589** (2021) 44-51.
2. Xiang S., Han Y., Song Z., Guo X., Zhang Y., Ren Z., Wang S., Ma Y., Zou W., Ma B., Xu S., Dong J., Zhou H., Ren Q., Deng T., Liu Y., Han G., Hao Y. - A review: Photonics devices, architectures, and algorithms for optical neural computing, Journal of Semiconductors. **42** (2021) 023105. DOI 10.1088/1674-4926/42/2/023105
3. Sunny F. P., Taheri E., Nikdast M., Pasricha S. - A Survey on Silicon Photonics for Deep Learning, J. Emerg. Technol. Comput. Syst. **17** (2021). DOI**:** 10.48550/arXiv.2101.01751
4. Deligiannidis L., Arabnia H. - Emerging Trends in Image Processing, Computer Vision and Pattern Recognition, Morgan Kaufmann, Leonidas Deligiannidis, Hamid Arabnia, 2014.
5. Papaioannou M., Plum E., Zheludev N. I. - All-Optical Pattern Recognition and Image Processing on a Metamaterial Beam Splitter, ACS Photonics. **4** (2017) 217-222. https://doi.org/10.1021/acsphotonics.6b00921
6. Azimi Fashi A., Vadjed Samiei M. H., Teixeira A. - Design of a visible light photonic chip for Haar transform based optical compression, Optik. **217** (2020) 164929. https://doi.org/10.1016/j.ijleo.2020.164929
7. Almeida L., Kumar N., Parca G., Tavares A., Lopes A., Teixeira A. - All-Optical image processing based on integrated optics. 16th International Conference on Transparent Optical Networks (ICTON), IEEE, (2014) 14526424, doi: 10.1109/icton.2014.6876660
8. Fashi A. A., Samiei M. H. V., Pinho C., Teixeira A. L. - Photonic Integrated Chip on TriPleX Platform for Realizing Optical Haar Transform and Compression in the Visible Spectrum, IEEE Journal of Quantum Electronics **57** (2021) 1-10. doi:10.1109/ jqe.2021.3102845
9. Siegman A. E. - Fiber Fourier optics, Optics Letters. **26** (2001) 1215-1217. DOI: 10.1364/ol.26.001215
10. Collings N. - Fourier Optics in Image Processing, CRC Press, 2020.
11. Le T. T. - The Design of Optical Signal Transforms Based on Planar Waveguides on a Silicon on Insulator Platform, International Journal of Engineering and Technology. **2** (2010) 245-251. doi:10.7763/ijet.2010.v2.128
12. Burrus S., Gopinath R. A., Guo H. - Introduction to Wavelets and Wavelet Transforms: A Primer. Prentice Hall, United States, 1998.

13. Azimi Fashi A., Vadjed Samiei M. H., Teixeira A. - Realization of visible light integrated circuits for all-optical haar transform, Optical and Quantum Electronics. **53** (2021) 364.
14. Bachmann M., Besse P. A., Melchior H. - General self-imaging properties in N × N multimode interference couplers including phase relations, Appl. Opt. **33** (1994) 3905. DOI: 10.1364/AO.33.003905
15. Heaton J. M., Jenkins R. M. - General matrix theory of self-imaging in multimode interference(MMI) couplers, IEEE Photonics Technology Letters. **11** (1999) 212-214. DOI**:** 10.1109/68.740707
16. Dominic F. G. G., Thomas P. F. - Eigenmode expansion methods for simulation of optical propagation in photonics: pros and cons, Integrated Optics: Devices, Materials, and Technologies VII. **4987** (10) (2003) 69-82. DOI: 10.1117/12.473173